Volume-3, Issue-1, January 2011, ISSN No.1998 - 7889 *Eastern University Journal*

A Review on Natural Convection Flow Along A Vertical Flat Plate

Amena Ferdousi*

Abstract

Natural convection flow along a vertical flat plate has been revisited with respect to thermal conductivity, magnetic parameter, heat conduction, joule heating, coupling conduction, conjugate heat transfer and heat generation and finally a comparative analysis of free convection flow along a vertical flat plate is presented in this work where analysis are broadly discussed in order to discover the results in all the case. The graphical presentation of the surface shear stress in terms of skin friction coefficient and the rate of heat transfer in terms of local Nusselt number, velocity as well as temperature profiles are shown graphically for a selection of parameters set, consisting of magnetohydrodynamic parameter M, heat generation parameter Q, thermal conductivity n, joule heating J, coupling conduction p, Prandtl number Pr.

Key words: joule heating, coupling conduction, conjugate heat transfer, heat generation, natural convection, magnetohydrodynamic.

1. Introduction

In this paper thermal conductivity, MHD, heat conduction and joule heating, coupling conduction, MHD and heat generation, and conjugate heat transfer on natural convection boundary layer flow along a vertical flat plate of a steady two dimensional viscous incompressible fluid is compared with various parameters. Throughout the work the behavior of all these parameters, their effects i.e., how the variations of the parameters are influencing the skin friction, nusselt number, velocity and temperature profiles.

Rahman et al. (2008) studied effects of temperature dependent thermal conductivity on magnetohydrodynamic (MHD) free convection flow along a vertical flat plate with heat conduction. Alim et al. (2008) studied joule heating effect on the coupling of conduction with magnetohydrodynamic free convection flow from a vertical flat plate. Mamun et al. (2008) studied conjugate heat transfer for a vertical flat plate with heat generation effect. Chang (2008) studied a numerical simulation of micro polar fluid flow along a flat plate with wall conduction and buoyancy effects. Me´ndez and Trevi˜no (2000) studied the conjugate conduction-natural convection heat transfer along a thin vertical plate with non-uniform internal heat generation. Hossain (1992) studied viscous and joule heating effects on MHD free convection flow with variable plate temperature. El-Amin (2003) studied combined effect of viscous dissipation and Joule heating on MHD forced convection over a non isothermal horizontal cylinder embedded in a fluid saturated

* *Assistant Professor, Faculty of Engineering and Technology, Eastern University*

porous medium. Ferdousi (2009) studied the effects of radiation on natural convection flow from a porous vertical plate in presence of heat generation. Hossain et al. (1999) studied the effect of radiation on free convection flow with variable viscosity from a porous vertical plate. Hossain et al. (1996) studied the effect of radiation on free convection flow from a porous vertical plate. None of the aforementioned works, compared thermal conductivity, MHD, heat conduction and joule heating, coupling conduction, MHD and heat generation, conjugate heat transfer on natural convection boundary layer flow along a vertical flat plate of a steady two dimensional viscous incompressible fluid.

In the present study, we observe the effects of thermal conductivity, magnetic parameter, heat conduction, joule heating; coupling conduction, conjugate heat transfer and heat generation and finally a comparative analysis of free convection flow along a vertical flat plate is presented. The results have been shown for different values of relevant physical parameters in graphs.

Nomenclatures

Pr Prandtl number
C_f Local skin friction coefficient
M Magnetohydrodynamic parameter
Q Heat generation parameter
(u, v) Dimensionless velocity components along the (x, y) axes
g Acceleration due to gravity
V Wall suction velocity
Nu Local Nusselt number
q_w Heat flux at the surface
J Joule heating
T Temperature of the fluid in the boundary layer
q_c Conduction heat flux.
R_d Radiation parameter
(x, y) Axis in the direction along and normal to the surface respectively
q_r Radiation heat flux
T_∞ Temperature of the ambient fluid
T_w Temperature at the surface
p Coupling conduction
n Thermal conductivity

Greek symbols

η Similarity variable
β Coefficient of thermal expansion
ξ Similarity variable
θ Dimensionless temperature function
θ_w Surface temperature parameter
τ_w Shearing stress

Subscripts

w wall conditions
∞ ambient temperature

2. Physical Model

Let us consider a steady, two-dimensional laminar incompressible free convection boundary layer flow along a side of a vertical flat plate of thickness b, insulated on the edges for which pure conduction takes place and with a temperature Tb maintained on the other side. The fluid properties are assumed to be constant in limited temperature range except for the influence of the density variations with temperature, which are considered only in body force term. The physical model and the co-ordinate system are shown in Fig. 1. The x-axis is taken along the vertical flat plate in the upward direction and the y-axis normal to the plate.

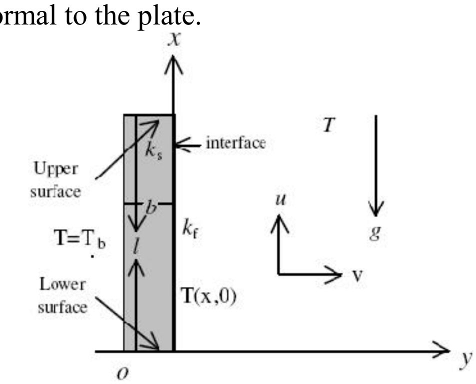

Fig. 1. Physical configuration and coordinates system.

3. Results and discussion

Effects of thermal conductivity, MHD and heat conduction:

Here effects of thermal conductivity, MHD and heat conduction for Prandtl number *Pr* have been shown:

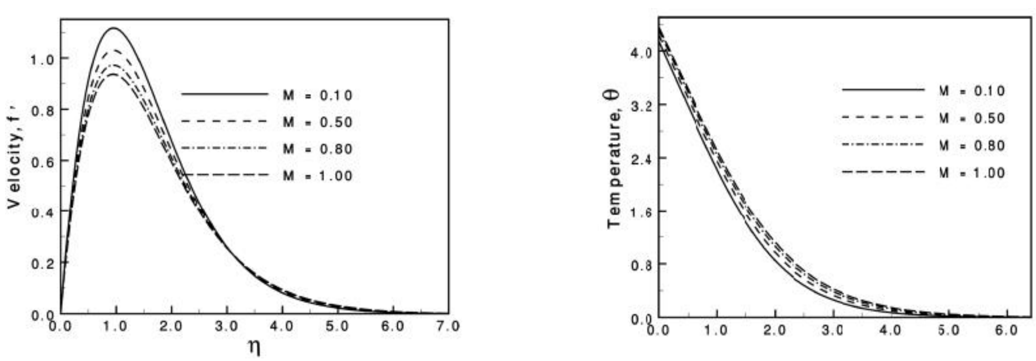

(a) (b)

Fig. 2. (a) Variation of velocity profiles and (b) variation of temperature profiles against η for different M with $n = 0.01$, $Pr = 0.733$ and $p = 0.25$.

The magnetic parameter decreases while the fluid velocity increases as shown in Fig. 2(a). From Fig. 2(b), it can be observed that the temperature within the boundary layer increases for the increasing *M*. The magnetic filed decreases the temperature gradient at the wall and increases the temperature in the flow region.

The thermal conductivity parameter on the velocity and temperature within the boundary layer with *M* = 0.10, *Pr* = 0.733 and *p* = 0.25 are shown in Fig. 3(a) and Fig. 3(b), respectively. It is seen from Fig. 3(a) and Fig. 3(b) that the velocity and temperature increase within the boundary layer with the increasing value of *n*. The maximum values of the velocity are 1.1166, 1.1466, 1.1768 and 1.2073 for n = 0.01, 0.03, 0.05 and 0.07, respectively and each of which occurs at η = 0.9423. It is observed that the velocity increases by 7.513% when n increases from 0.01 to 0.07. Furthermore, the maximum values of the temperature are 4.1430, 4.2533, 4.3632 and 4.4725 for *n* = 0.01, 0.03, 0.05 and 0.07, respectively and each of which occurs at the surface. It is observed that the temperature increases by 2.593% when n increases from 0.01 to 0.07. Fig. 4(a) and Fig. 4(b) illustrate the velocity and temperature profiles for different 518 Effects of Temperature Dependent Thermal Conductivity on Magnetohydrodynamic values of Prandtl number Pr with *M* = 0.10, *n* = 0.01 and p = 0.25. From Fig. 4(a), it can be observed that the velocity decreases with the increasing *Pr*. It is also observed that the maximum values of the velocity are 1.1184, 0.7830, 0.6187 and 0.5274 for *Pr* = 0.733, 1.73, 2.97 and 4.24, respectively which occurs at η = 0.9423, 0.8881, 0.8353 and 0.8353, respectively. It is seen that the velocity decreases by 52.843%when *Pr* increases from 0.733 to 4.24. Furthermore, the maximum values of the temperature are observed to be 4.1464, 3.5023, 3.1633 and 2.9645 for Pr = 0.733, 1.73, 2.97 and 4.24, respectively and each of which occurs at the surface. It is shown that the temperature decreases by 6.285% when *Pr* increases from 0.733 to 4.24.

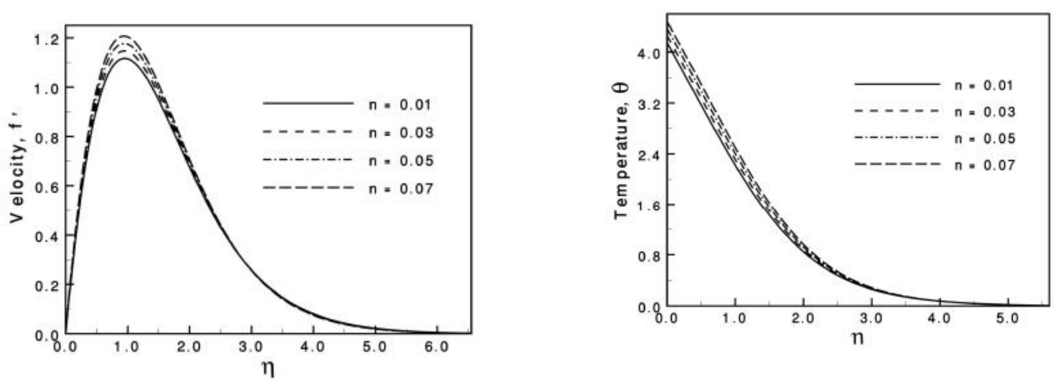

(a) (b)

Fig. 3. (a) Variation of velocity profiles and (b) variation of temperature profiles against η for varying of *n* with *M* = 0.10, *Pr* = 0.733 and *p* = 0.25.

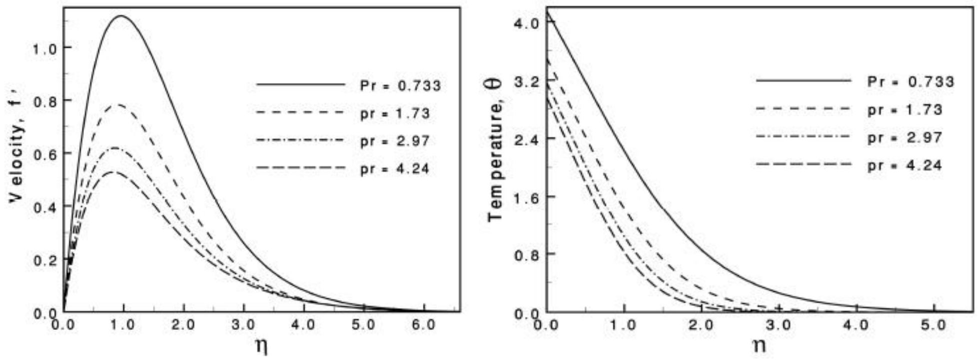

(a) (b)

Fig. 4. (a) Variation of velocity profiles and (b) variation of temperature profiles against η for varying of *Pr* with $M = 0.10$, $n = 0.01$ and $p = 0.25$.

The conjugate conduction parameter *p* for $M = 0.10$, $n = 0.01$ and $Pr = 0.733$ on the velocity and temperature profiles are shown in Fig. 5(a) and Fig. 5(b), respectively. From Fig. 5(a) it can be noted that the velocity is retarded for the higher values of p. From Fig. 5(b), it can be seen that the temperature of the fluid within the boundary layer decreases for the increasing *p*. The temperature profile shifts downwards in the fluid and eventually the velocity of the fluid within the boundary layer decreases.

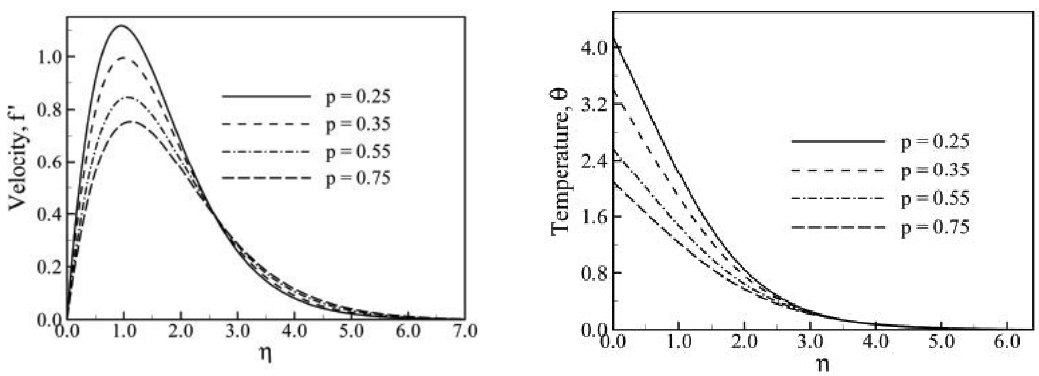

(a) (b)

Fig. 5. (a) Variation of velocity profiles and (b) variation of temperature profiles against η for varying of *p* with $M = 0.10$, $n = 0.01$ and Pr = 0.733.

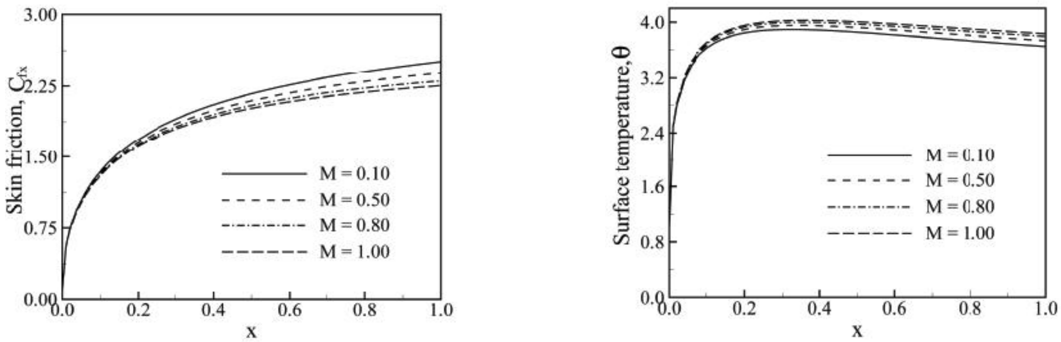

(a) (b)

Fig. 6. (a) Variation of skin friction coefficients and (b) variation of surface temperature distributions against x for varying of *M* with $n = 0.01$, $Pr = 0.733$ and $p = 0.25$.

The local skin friction coefficient C_{fx} and surface temperature $\theta(\text{x}, 0)$ for different values of *M* with $Pr = 0.733$, $n = 0.01$ and $p = 0.25$ at different positions of *x* are illustrated in Fig. 6(a) and Fig. 6(b), respectively. It is observed from Fig. 6(a) that the increase value of the Magnetic parameter *M* leads to a decrease in the skin friction factor. Again Fig. 6(b) shows that the surface temperature $\theta(\text{x}, 0)$ increases due to the increased value of the magnetic parameter *M*. The magnetic field acting against the flow reduces the skin friction and produces the temperature at the interface.

Fig. 7(a) and Fig. 7(b) illustrate the effect of the thermal conductivity variation parameter on the skin friction coefficient and surface temperature distribution against *x* with $M = 0.10$, $Pr = 0.733$ and $p = 0.25$. From Fig. 7(a) it is seen that the skin friction coefficient increases along the upward direction of the plate for a particular value of *n*. It is also seen that the skin friction factor increases for the increasing n. From Fig. 7(b) it is seen that the surface temperature increases for the increasing *n*. This is to be expected because the higher value of the thermal conductivity variation parameter accelerates the fluid flow and increases the temperature as mentioned in Fig. 3(a) and 3(b),

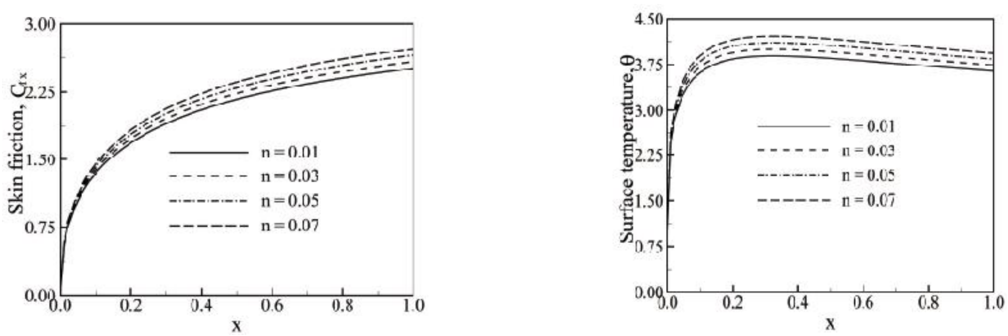

(a) (b)

Fig. 7. (a) Variation of skin friction coefficients and (b) variation of surface temperature distributions against *x* for varying of *n* with $M = 0.10$, $Pr = 0.733$ and $p = 0.25$.

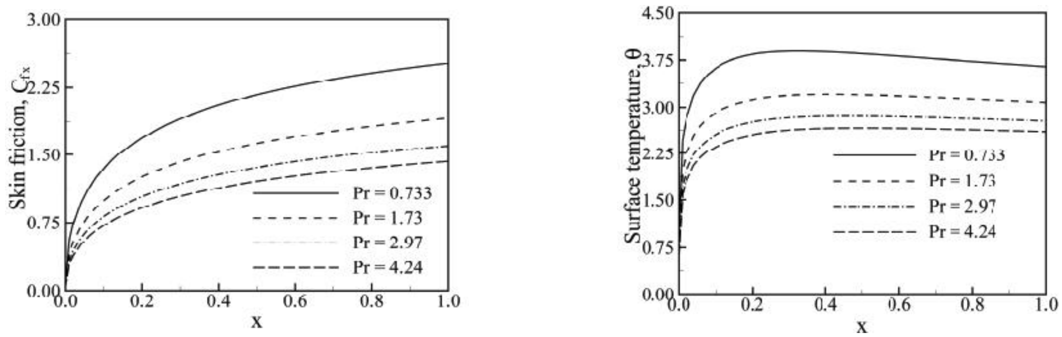

Fig. 8. (a) Variation of skin friction coefficients and (b) variation of surface temperature distributions against *x* for varying of *Pr* with *M* = 0.10, *n* = 0.01 and *p* = 0.25.

Fig. 8(a) and Fig. 8(b) deal with the effect of Prandtl number on the skin friction coefficient and surface temperature distribution against *x* with *M* = 0.10, *n* = 0.01 and *p* = 0.25. It can be observed from Fig. 8(a) that the skin friction coefficient increases monotonically for a particular value of *Pr*. It can also be noted that the skin friction coefficient decreases for the increasing *Pr*. From Fig. 8(b), it can be seen that the surface temperature distributions decrease owing to the increase of the Prandtl number. Fig. 9(a) and Fig. 9(b) deal with the effect of the conjugate conduction parameter on the local skin friction factor and the surface temperature with *M* = 0.10, *n* = 0.01 and *Pr* = 0.733. From Fig. 9(a) it is observed that the skin friction decreases for the increasing *p*. Moreover, the skin friction co-efficient increases for a particular value of *p* along the upward direction of the plate. Again from Fig. 9(b) it is seen that the surface temperature decreases for the increasing *p*. Furthermore, the surface temperature increases in a certain region and then decreases along the positive *x*-direction. This is because the higher value of *p* reduces the fluid flow and decreases the temperature as mentioned in Fig. 5(a) and Fig. 5(b), respectively.

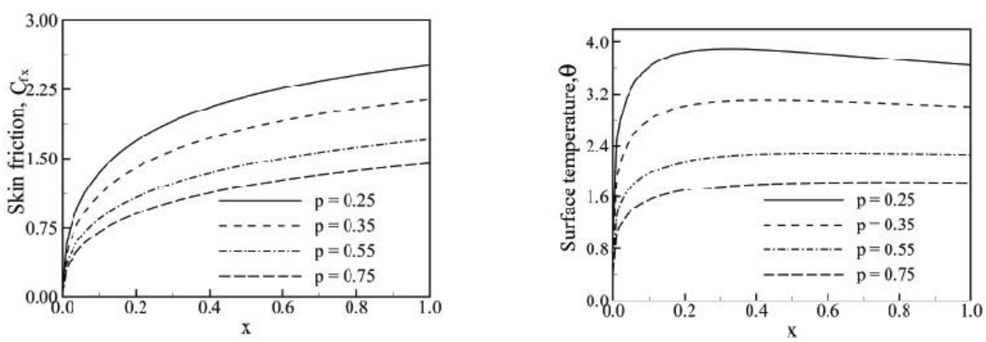

(a) (b)

Fig. 9. (a) Variation of skin friction coefficients and (b) variation of surface temperature distributions against *x* for varying of *p* with *M* = 0.10, *n* = 0.01 and *Pr* = 0.733

Effects of joule heating, coupling conduction and MHD:

Here effects of joule heating, coupling conduction, MHD for Prandtl number *Pr* have been shown:

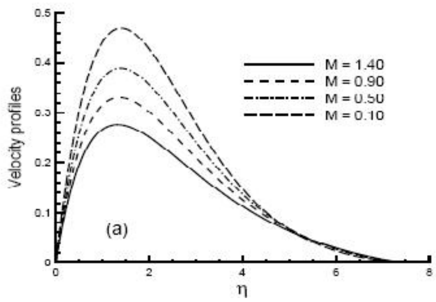

(a)

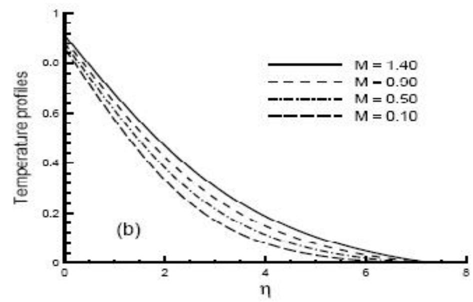

(b)

Fig. 10. (a) Velocity and (b) temperature profiles for different values of magnetic parameter M against η with other fixed values $Pr = 0.72$, $J = 0.07$.

Figs. 10(a), (b) show results for the velocity and temperature profiles, for different small values of magnetic parameter M (M = 0.10, 0.50, 0.90, 1.40) plotted against η at Pr = 0.72 and J = 0.07. It is seen from Fig. 10(a) that the velocity profile is decreases when the value of magnetic parameter M increases. But near the surface of the plate velocity increases significantly and then decreases slowly and finally approaches to zero. The maximum values of the velocity are 0.2765, 0.3302, 0.3895 and 0.4694 for M = 1.40, 0.90, 0.50, 0.10 respectively which occur at η = 1.3025 for the first maximum value and η = 1.3693 for others maximum values. Here the velocity decreases by 41.086% as M increases from 0.10 to 1.40. Also the temperature field increases for increasing values of magnetic parameter M in Fig. 10(b). Here it is seen that the local maximum values of the temperature profiles are 0.9132, 0.8965, 0.8803, 0.8615 for M = 1.40, 0.90, 0.50, 0.10 respectively and each of which occurs at the surface. Thus the temperature profiles increase by 5.67% as M increases from 0.10 to 1.40.

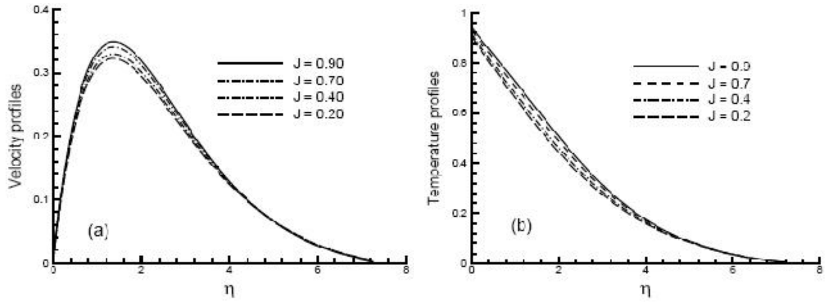

(a) (b)

Fig. 11 (a) Velocity and (b) temperature profiles for different values of Joule heating parameter *J* against η with other fixed values *Pr* = 0.72, *M* = 1.0.

Figs. 11(a) and 11(b) represent, respectively, the velocity and the temperature profiles for different values of the Joule heating parameter *J* for particular values of the Prandtl number and the magnetic parameter *M*. We observe from Fig. 11(a), that an increase in the Joule heating parameter *J*, is associated with a considerable increase in velocity profiles but near the surface of the plate the velocity increases and becomes maximum and then decreases and finally approaches to zero asymptotically. The maximum values of the velocity are 0.3490, 0.3412, 0.0.3299, 0.3226 for *J* = 0.90, 0.70, 0.40, 0.20 respectively and each of which occurs at η = 1.3693. Here we observe that the velocity increases by 7.57% as J increases from0.20 to 0.90. However Fig. 11(b) shows the temperature profiles against η for some values of the Joule heating parameter *J (J* = 0.90, 0.70, 0.40, 0.20) Clearly it is seen that the temperature distribution increases owing to increasing the values of the Joule heating parameter *J* and the maximum is at the adjacent of the plate wall. The local maximum values of the temperature profiles are 0.9408, 0.9302, 0.9153, 0.9059 for *J* = 0.90, 0.70, 0.40, 0.20 respectively and each of which attains at the surface. Thus the temperature profiles increase by 3.71% as J increases from 0.20 to 0.90.

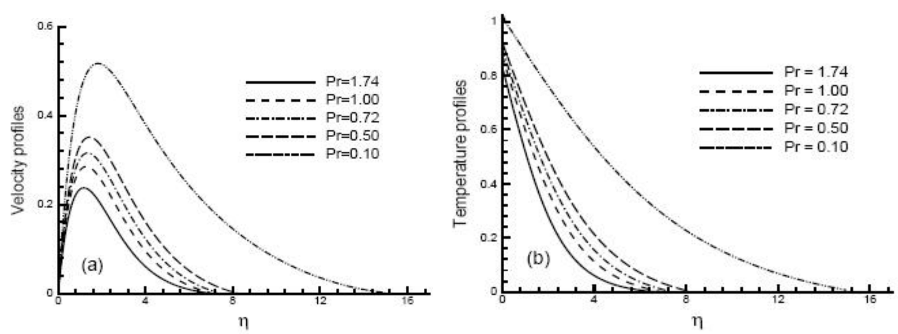

(a) (b)

Fig. 12. (a) Velocity and (b) temperature profiles for different values of Prandtl number Pr against η with other fixed values J = 0.005, M = 1.0

Fig. 12 (a) and (b) illustrates the velocity and temperature profiles for different values of Prandtl number in presence of the magnetic parameter *M* and Joule heating parameter *J*. From Fig. 12(a), we may conclude that the velocity profile is influenced significantly and decreases when the value of the Prandtl number *Pr* increases. The maximum values of the velocity are 0.2373, 0.2852, 0.3156, 0.3513, 0.5169 for *Pr* = 1.74, 1.00, 0.72, 0.50, 0.10

respectively which occur at η = 1.1752 for the first maximum value, η = 1.3025 for the second maximum value, η = 1.3693 for the third maximum value, η = 1.4382 for the fourth maximum value and at η = 1.8198 for the last maximum value. The maximum values of the temperature are 0.8310, 0.8732, 0.8972, 0.9232, 1.0249 for *Pr* = 1.74, 1.00, 0.72, 0.50, 0.10 respectively which occurs at the wall of the plate surface. Here it is found that the velocity and temperature profiles decrease by 54.1% and 18.92% respectively while Pr increases from 0.10 to 1.74.

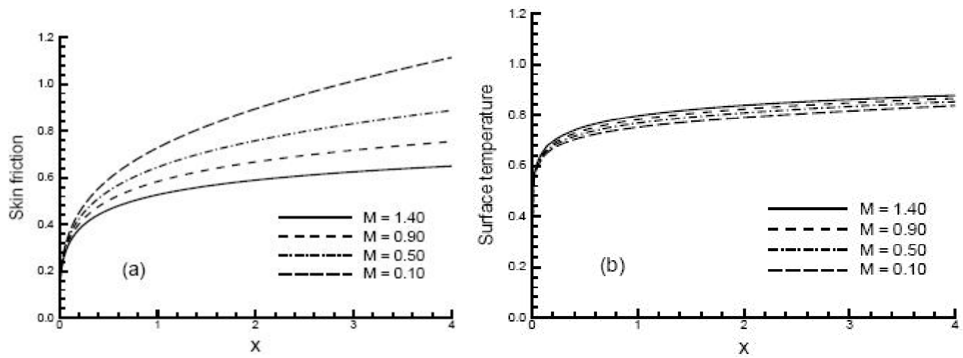

(a) (b)

Fig. 13. (a) Skin friction and (b) surface temperature against *x* for different values of magnetic parameter *M* with fixed parameter *Pr* = 0.72, *J* = 0.07.

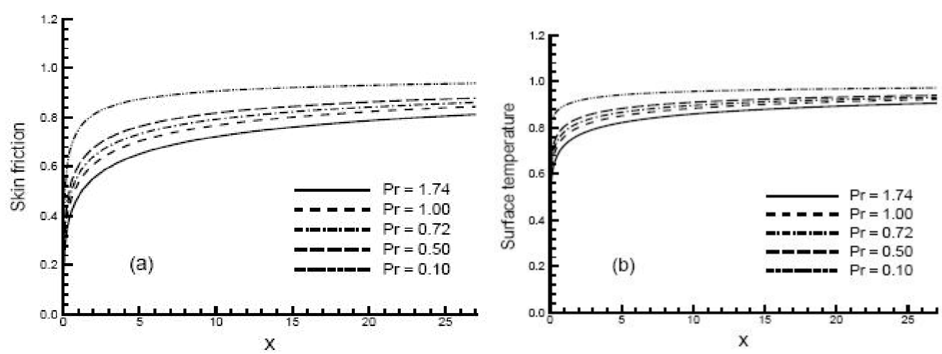

(a) (b)

Fig.14. (a) Skin friction and (b) surface temperature against *x* for different values of Prandtl number *Pr* with *M* = 1.0, *J* = 0.005.

Figs. 14(a), (b) illustrate the variation of skin-friction $f^{''}(x, 0)$ and surface temperature distribution θ(x, 0) against x for different values of magnetic parameter M (M = 1.40, 0.90, 0.50, 0.10). It is seen from Fig. 14(a) that the skin-friction $f^{''}(x, 0)$ is decreases when the magnetic parameter, M increases. It is also observed in Fig. 14(b), the surface temperature $\theta(x, 0)$ distribution increases while M increases. The value of the skin-friction $f^{''}(x, 0)$ decreases by 23.53% and the surface temperature distribution $\theta(x, 0)$ decreases by 4.33% while the magnetic parameter M increasing from 0.10 to 1.40.

Effect of heat generation, conjugate heat transfer parameter:

Here effect of heat generation, conjugate heat transfer Q for Prandtl number Pr have been shown:

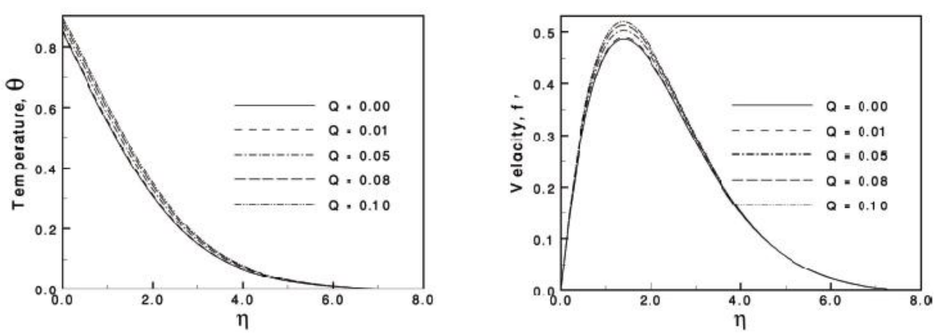

(a) (b)

Fig. 15. (a) Variation of temperature profiles and (b) variation of velocity profiles against η for varying of Q with p = 1.0 and Pr = 0.73.

In Fig. 15 (a) and (b) for increasing Q both the temperature and velocity profile increase. The effect of the conjugate conduction parameter on the temperature and the velocity within the boundary layer with Q = 0.01 and Pr = 0.73 is shown in Figs. 16(a) and (b), respectively. The temperature and the velocity also decrease with the increasing p.

In Fig. 17, different values of Prandtl number with Q = 0.01, and p = 1 are considered for the velocity and temperature distributions. The overall temperature profiles also shift downwards with the increasing Pr as observed in Fig. 17(a). The physical fact that the thermal boundary layer thickness decreases with increasing Pr supports the result. Moreover, for a given Pr the surface temperature increases along the positive direction of x. The variation of the local skin friction coefficient C_{fx} and local rate of heat transfer N_{ux} with Pr = 0.73 and p = 1.0 for different values of Q at different positions are illustrated in Fig. 18(a) and (b), respectively. The increased skin friction coefficients with the increasing Q represent this phenomenon as illustrated in Fig. 18(a). Accordingly, the heat transfer rate from the surface decreases as shown in Fig. 18(b) The variation of the reduced local skin friction coefficient C_{fx} and the local rate of heat transfer N_{ux} for different values of p with res pect to x are shown in Fig. 19(a) and (b), respectively where Q = 0.01 and Pr = 0.73. The increased value of p decreases the velocity of the fluid within the boundary layer, as mentioned in Fig. 16(b), and decreases the viscosity of the fluid. As a result the corresponding skin friction coefficient decreases as shown in Fig. 19(a). On the other hand, from Fig. 19(b), it can be observed that an increase in the p is associated with a decrease in the local rate of heat transfer. Fig. 20(a) and (b) deal with the effect of Pr on the skin friction coefficient and the rate of heat transfer against x with Q = 0.01 and p = 1.0. Fig. 20(a) shows that an increase in the Prandtl number Pr is associated with a decrease in the skin friction coefficient and from Fig. 20(b) it is seen that an increase in the Prandtl number Pr is associated with an increase in the rate of heat transfer

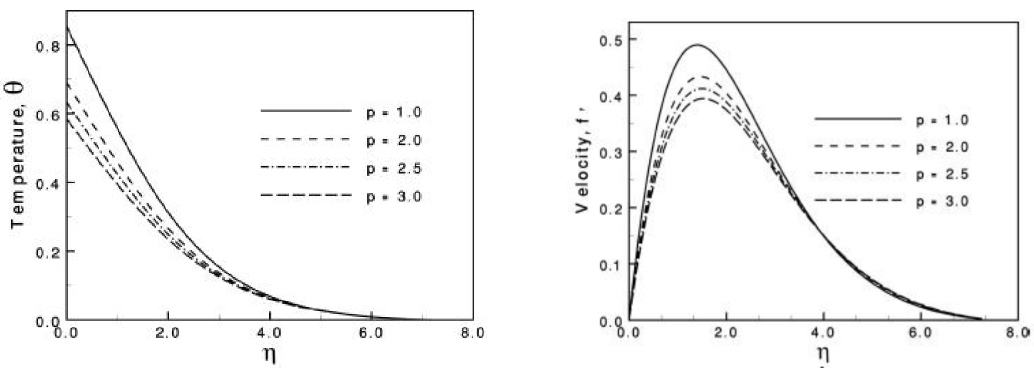

(a) (b)

Fig. 16. (a) Variation of temperature profiles and (b) variation of velocity profiles against η for varying of p with Q = 0.01 and Pr = 0.73.

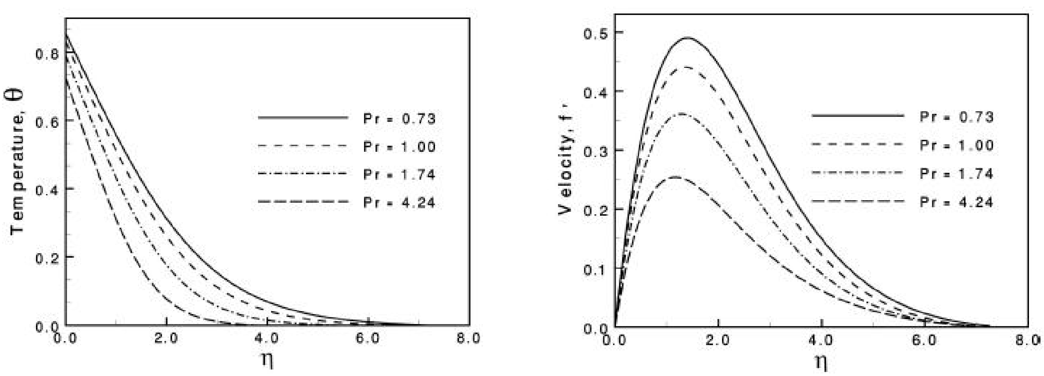

(a) (b)

Fig. 17. (a) Variation of temperature profiles and (b) variation of velocity profiles against η for varying of Pr with Q = 0.01 and p = 1.0.

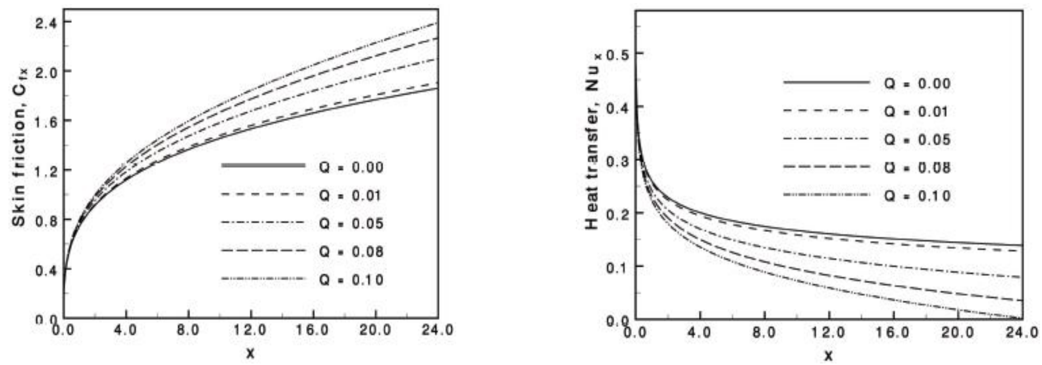

(a) (b)

Fig. 18. (a) Variation of skin friction coefficients and (b) variation of rate of heat transfer against *x* for varying of *Q* with *p* = 1.0 and *Pr* = 0.73.

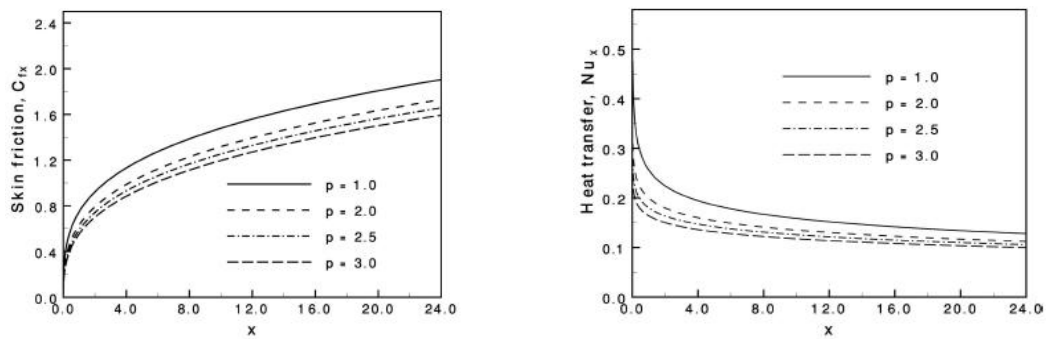

(a) (b)

Fig. 19. (a) Variation of skin friction coefficients and (b) variation of rate of heat transfer against *x* for varying of *p* with *Q* = 0.01 and *p* = 1.0.

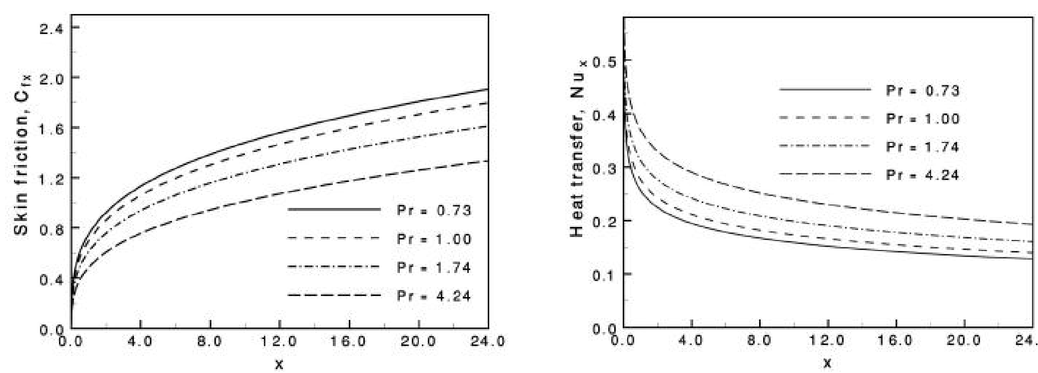

(a) (b)

Fig. 20. (a) Variation of skin friction coefficients and (b) variation of rate of heat transfer against *x* for varying of *Pr* with *Q* = 0.01 and *p* = 1.0.

4. Conclusion

The effect of thermal conductivity, MHD, heat conduction, coupling conduction, heat generation for Prandtl number *Pr* have been observed for different values of relevant physical parameters. From the present investigation the following conclusions may be drawn:

- The velocity within the boundary layer increases for decreasing *M, Pr* and *p* but for increasing *n*.
- The velocity is increasing for increasing value of the Joule heating parameter *J* and for, the decrease of the magnetic parameter *M* and the Prandtl number *Pr*.
- The velocity of the fluid increase with the increasing heat generation parameter while as it is described above for the *Pr* and *p*.
- The temperature is increasing for increasing value of the Joule heating parameter *J* and for the increase of the magnetic parameter *M* and the Prandtl number *Pr*.
- The temperature within the boundary layer increases for the increasing *M* and *n* but for decreasing *Pr* and *p*.
- The temperature of the fluid increases with the increasing heat generation parameter and as it is described above for *Pr* and *p*.
- The skin friction coefficient decreases for the increasing *M, Pr* and *p* but for decreasing *n*.
- The skin friction is as it is described above for the magnetic parameter *M* and the Prandtls number *Pr*.
- The skin friction at the interface increase with the increasing heat generation parameter as it is described above for *Pr* and *p*.
- The rate of heat transfer decreases with the increasing heat generation parameter, conduction parameter and the decreasing Prandtl number.
- An increase in the values of the thermal conductivity variation parameter n, magnetic parameter *M* lead to an increase in the surface temperature. The surface temperature decreases for the increasing *Pr* and conjugate conduction parameter *p*.

References

M.M. Rahman, A.A. Mamun, M.A. Azim, M.A. Alim,"Effects of temperature dependent thermal conductivity on magnetohydrodynamic (MHD) free convection flow along a vertical flat plate with heat conduction". *Nonlinear Analysis: Modelling and Control*, 2008, Vol. 13, No. 4, 513–524.

M.A. Alim, Md. M. Alam, Abdullah-Al-Mamun, "Joule heating effect on the coupling of conduction with magnetohydrodynamic free convection flow from a vertical flat plate". *Nonlinear Analysis: Modelling and Control*, 2008, Vol. 12, No. 3, 307–316.

A.A. Mamun, Z.R. Chowdhury, M.A. Azim, M.A. Maleque, "Conjugate heat transfer for a vertical flat plate with heat generation effect". *Nonlinear Analysis: Modelling and Control*, 2008, Vol. 13, No. 2, 213–223.

Cheng Long Chang, "A numerical simulation of micro polar fluid flow along a flat plate with wall conduction and buoyancy effects", *J. Appl. Phys. D*, 39, pp. 1132–1140, 2006.

F. Meńdez, C. Treviňo, "The conjugate conduction-natural convection heat transfer along a thin vertical plate with non-uniform internal heat generation", *International Journal of Heat and Mass Transfer*, 43, pp. 2739–2748, 2000.

M.A. Hossain, "Viscous and Joule heating effects on MHD free convection flow with variable plate temperature", *International Journal of Heat and Mass Transfer*, 35(12), pp. 3485–3487, 1992.

M. F. El-Amin, "Combined effect of viscous dissipation and Joule heating on MHD forced convection over a non isothermal horizontal cylinder embedded in a fluid saturated porous medium", *Journal of Magnetism and Magnetic Materials*, 263(3), pp. 337–343, 2003.

Cebeci T., Bradshaw P., 1984, Physical and *Computational Aspects of Convective Heat* Transfer, New York, Springer-Verlag, New York, pp. 497.

Ferdousi Amena, 2009, "Numerical study of the effects of radiation on natural convection flow from a porous vertical plate in presence of heat generation", *M.Phil Thesis, Department of Mathematics, Bangladesh University of Engineering and Technology (BUET), Dhaka, Bangladesh.*

Hossain Md. A, Alim Md. A., Rees D. A. S., 1999, "The effect of radiation on free convection flow from a porous vertical plate", *International Journal of Heat and Mass Transfer, ISSN: 0017-9310, 42, pp. 81-91.*

Hossain Md. A, Takhar H. S, 1996, "Radiation effect on mixed convection along a vertical plate with uniform surface"*, International Journal of Heat and Mass Transfer*, ISSN: 0735-1933, 31, pp. 243-248.

Keller H. B., 1978, "Numerical methods in boundary layer theory", *Annual Review of Fluid Mechanics*, ISSN: 0066-4189, ISBN: 0-8243-0738-0, 10, pp. 417-433.